Geophysical Research Letters

RESEARCH LETTER
10.1029/2026GL123617

Regulatory Factors of the Morning Peak of Summer Regional Precipitation Events Over the Middle and Lower Yangtze River Basin, China

Rongchang Wu[1], Anning Huang[1,2], Danqing Huang[1], Chunlei Gu[1], and Shanshan Li[1,3]

[1]School of Atmospheric Sciences, Nanjing University, Nanjing, China, [2]Qinghai Lake Comprehensive Observation Research Station, Chinese Academy of Sciences, Gangcha, China, [3]China Meteorological Administration Basin Heavy Rainfall Key Laboratory & Hubei Key Laboratory for Heavy Rain Monitoring and Warning Research, Institute of Heavy Rain, China Meteorological Administration, Wuhan, China

Abstract The diurnal variation of regional precipitation events (RPE) over the Middle and Lower Yangtze River Basin (MLYRB) significantly affects human activities and serves as a key reference for weather forecasting. Here, the diurnal variation of summer RPE over MLYRB under two monsoonal synoptic types and their regulatory factors have been addressed. Results indicate that the morning peak of RPE is closely associated with the southwesterly low-level jet (SLLJ) and western Pacific subtropical high (WPSH). Specifically, SLLJ begins to accelerate at night driven by the ageostrophic wind, facilitating the development of the precipitation system. Subsequently, the morning westward expansion of WPSH provides large-scale circulation forcing, leading to the strongest lower-tropospheric convergence and mid-tropospheric ascending motion over MLYRB, thereby generating the morning peak of RPE. Additionally, RPE are accompanied by significant frontogenesis, and deformation frontogenesis plays a more significant role than divergence frontogenesis in regulating the morning peak of RPE.

Plain Language Summary The diurnal variation of summer regional precipitation events (RPE) over the Middle and Lower Yangtze River Basin (MLYRB) greatly affects human activities, lives, and property, but the regulatory factors associated with diurnal variations of RPE remain unclear. This study demonstrates the relevant mechanisms driving the diurnal variation of RPE over MLYRB in summer under two monsoonal synoptic types. Results indicate that the morning peak of RPE over MLYRB is closely associated with the southwesterly low-level jet (SLLJ) and western Pacific subtropical high (WPSH). At night, SLLJ accelerates under the influence of ageostrophic wind, supporting the development of precipitation systems. As WPSH extends westward in the morning, the strongest low-tropospheric convergence and mid-tropospheric ascending motion occur over MLYRB, resulting in a distinct morning peak of RPE. Moreover, the deformation frontogenesis plays a more significant role than divergence frontogenesis in regulating the diurnal variation of RPE. Findings of this study may deepen our understanding of the mechanisms behind the morning peak of precipitation over MLYRB, providing scientific references on the sub-daily scale for more accurate precipitation forecasting.

Key Points:

- The morning peak of regional precipitation events in Middle and Lower Yangtze River Basin is associated with the southwesterly low-level jet
- The strengthened low-level relative vorticity, convergence and mid-level ascending motion contribute to the morning peak of precipitation
- The deformation frontogenesis plays a more significant role than divergence frontogenesis in regulating the morning peak of precipitation

Supporting Information:

Supporting Information may be found in the online version of this article.

Correspondence to:

A. Huang,
anhuang@nju.edu.cn

Citation:

Wu, R., Huang, A., Huang, D., Gu, C., & Li, S. (2026). Regulatory factors of the morning peak of summer regional precipitation events over the middle and lower Yangtze River Basin, China. *Geophysical Research Letters*, *53*, e2026GL123617. https://doi.org/10.1029/2026GL123617

Received 9 APR 2026
Accepted 19 JUN 2026

Author Contributions:

Conceptualization: Anning Huang
Data curation: Anning Huang, Danqing Huang
Formal analysis: Rongchang Wu, Anning Huang
Funding acquisition: Anning Huang
Investigation: Rongchang Wu, Anning Huang
Methodology: Rongchang Wu
Project administration: Anning Huang
Resources: Rongchang Wu, Anning Huang, Danqing Huang, Shanshan Li
Software: Rongchang Wu, Chunlei Gu

1. Introduction

The diurnal variation of precipitation, as significant fundamental feature of precipitation, plays a crucial role in the Earth system's water and energy cycles (Ali & Mishra, 2018; Ruane, 2010; Sui et al., 2025). The diurnal variation of precipitation involves numerous complex physical mechanisms, such as topographical forcing, multiscale weather system interactions and cloud microphysics processes, which jointly result in pronounced regional differences (Gong et al., 2018; Minobe et al., 2020; Pan & Chen, 2019). Advances in station, satellite, and multi-source fusion precipitation data have greatly improved our understanding of precipitation diurnal variation on global scale, providing crucial reference for water resource management and weather forecasting (Chen et al., 2012, 2024; Dai, 2024; Hayden & Liu, 2021). In most continental regions, the precipitation peaks in the afternoon as solar heating during the daytime leads to atmospheric instability and increased convective activity (Pan et al., 2021; Rickenbach et al., 2015; Yang & Smith, 2008), whereas over marine regions, the precipitation exhibits early morning peak due to mesoscale systems typically initiating around midnight and maturing in the early morning (Nesbitt & Zipser, 2003; Qiao & Liang, 2016; Song et al., 2024).

Supervision: Anning Huang, Danqing Huang
Validation: Rongchang Wu, Anning Huang, Chunlei Gu
Visualization: Rongchang Wu
Writing – original draft: Rongchang Wu, Anning Huang, Danqing Huang, Chunlei Gu, Shanshan Li
Writing – review & editing: Rongchang Wu, Anning Huang, Danqing Huang, Chunlei Gu, Shanshan Li

The diurnal variation of precipitation in the middle and lower Yangtze River basin (MLYRB) exhibits diverse patterns, driven by East Asian summer monsoon, mountain-plain solenoid circulation, mesoscale convective systems and urbanization (Li et al., 2024; Tang et al., 2022; Wang et al., 2014; Zhang & Sun, 2017). Regional precipitation events (RPE), typically triggered by weather systems characterized by large spatial scales and long duration (Yu et al., 2015), occur most frequently over MLYRB during June and July (the Meiyu rainy season) and contribute significantly to the total summer precipitation (Guan et al., 2020; Wu et al., 2025). Some studies based on case analyses have shown that the strengthened low-level wind is a key factor for the diurnal variation of precipitation, bringing the most abundant moisture several hours ahead of the precipitation peak (Fu et al., 2019; Xue et al., 2018; Zeng et al., 2019). Moreover, convective systems, as the primary contributors to rainfall over MLYRB, are frequently embedded in stratiform clouds and exhibit morning peak (Liu et al., 2005; Yang et al., 2020; Zhang et al., 2023, 2025). However, most studies have focused on analyzing the characteristics of diurnal variation or investigating the mechanisms of precipitation event cases (Yu et al., 2007; Zeng et al., 2019; Zhang & Sun, 2017), lacking a comprehensive understanding regarding the morning peak of precipitation over MLYRB at the climatological scale.

Previous studies have revealed the driving factors of heavy precipitation over MLYRB, including large-scale circulation anomalies and frontogenesis dynamics (Cao et al., 2019; Hu et al., 2021; Li & Lu, 2018; Xue et al., 2025). The confrontation between cold and warm air frequently generates quasi-stationary frontal system over MLYRB, providing favorable dynamic conditions for precipitation (Du et al., 2020; Li et al., 2023; Yang et al., 2025; Zeng et al., 2023). Moreover, a strong positive correlation exists between frontogenesis and precipitation during the Meiyu period, and the effects of different frontogenesis terms on precipitation vary significantly (Hou & Guan, 2013; Yang et al., 2015; Yuan et al., 2020). However, the effects of these mechanisms on the diurnal variation of precipitation over MLYRB remain unclear.

Additionally, studies based on single-station precipitation events indicate that longer-duration precipitation events are the primary factor contributing to the morning peak in precipitation (Liu et al., 2021; Yao et al., 2022). However, single-station analysis without considering the spatiotemporal evolution of precipitation leads to incomplete identification of precipitation processes and insufficient understanding of their physical mechanisms. Wu et al. (2025) have identified spatiotemporally continuous RPE in MLYRB during summer over the past decades. The composite analysis of precipitation and environmental fields during RPE can effectively eliminate interference signals from non-precipitation and local precipitation periods, providing a new perspective for understanding the morning peak of precipitation. Wu et al. (2025) employed spectral clustering to classify the dominant synoptic types triggering RPE into three types, including two monsoonal synoptic types and landfalling tropical cyclone synoptic type. These findings indicated that RPE dominates the morning peak of total precipitation in summer, but the mechanisms underlying their diurnal variations have not been explored. Therefore, this study aims to explore the influence of atmospheric dynamic and thermodynamic factors on the diurnal variation of RPE over MLYRB in summer and the underlying physical mechanisms. Findings of this study may deepen the understanding of precipitation formation mechanisms on the sub-daily scale.

2. Data and Methods

2.1. Data

In the study, the hourly precipitation data from rainfall gauge station in the boreal summer from 1980 to 2022 over MLYRB provided by the China Meteorological Administration is used to analyze the diurnal variation of RPE (300 station positions shown in Figure 1). To investigate the diurnal variations of environmental conditions, the fifth generation European Center for Medium-range Weather Forecasts atmospheric reanalysis (ERA5) hourly dataset at different pressure levels with a horizontal resolution of 0.25° is employed (Hersbach et al., 2020). The variables include geopotential height, specific humidity, temperature, vertical velocity, zonal wind (U) and meridional wind (V). Corresponding to hourly precipitation data, ERA5 data is converted from coordinated universal time (UTC) to local solar time (LST, UTC + 8 hr).

2.2. Definition of Diurnal Variation of RPE

The identification of RPE and clustering of synoptic types in this study are based on Wu et al. (2025), with a brief description provided in Text S1 of Supporting Information S1. The diurnal variations of precipitation amount (PA), precipitation frequency (PF), and precipitation intensity (PI) for hourly regional precipitation are defined

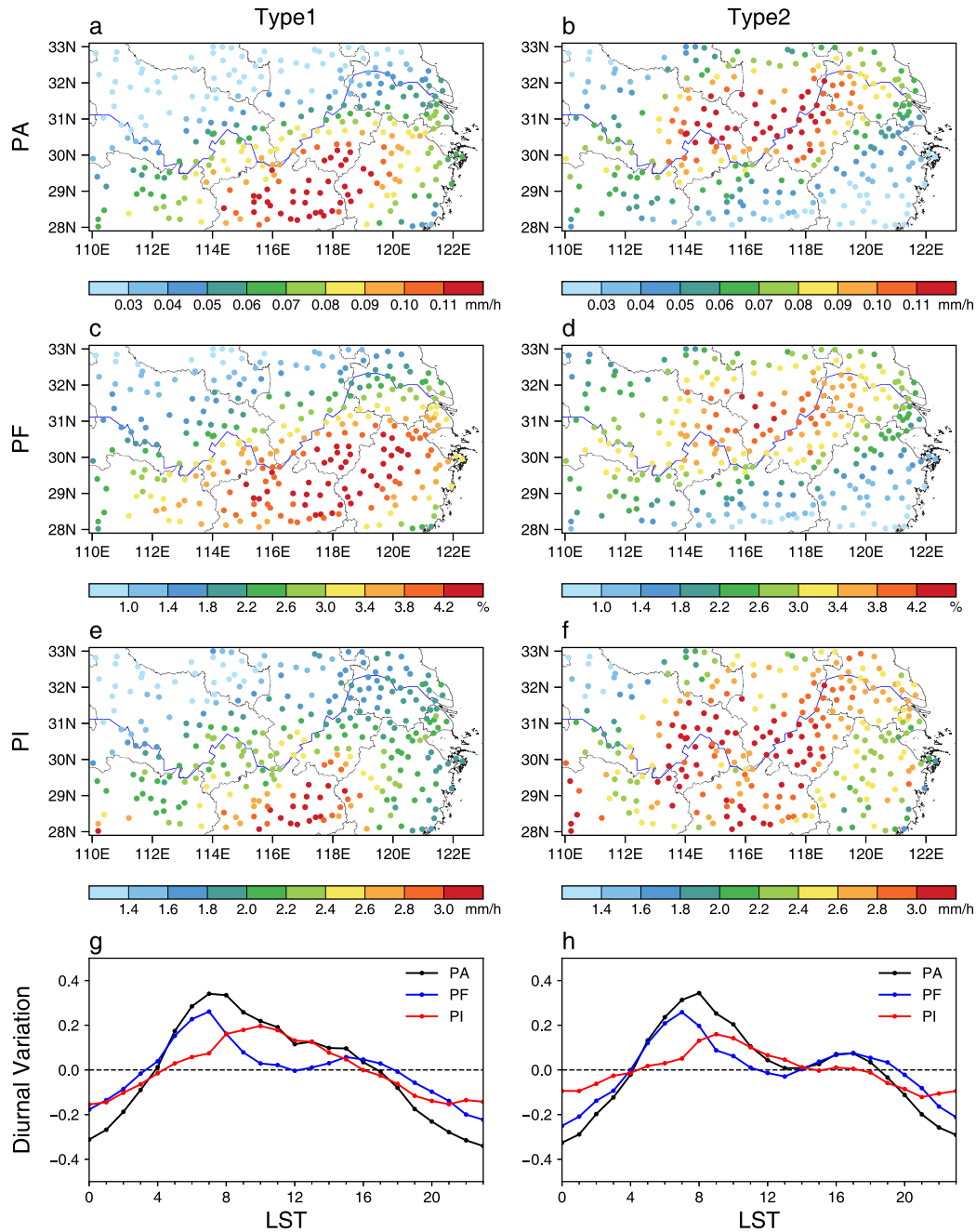

Figure 1. The spatial distribution of (a, b) PA (unit: mm/h) (c, d) PF (unit: %) and (e, f) PI (unit: mm/h) for the RPE under two monsoonal synoptic types over MLYRB during the summers of 1980–2022. The normalized diurnal variation of climatic mean PA, PF and PI in summers of 1980–2022 regionally averaged over MLYRB (g, h).

according to previous studies (Wu et al., 2018; Yu et al., 2014). The total hours for a specific hour of a day (00:00-23:00 LST) in the 43 summers is 3,956 hr (92 days/summer × 43 summers). At the specific hour of a day the total hours of RPE is denoted by h, the number of stations with precipitation (hourly precipitation ≥0.1 mm) is N_t and the precipitation at the i station is $p_{i,t}$ $(i = 1,2,\cdots,N_t)$ at the time t $(t = 1,2,\ldots,\text{h})$. The regional means of PA, PF, and PI over the MLYRB at a specific hour of a day are calculated as follows:

$$\text{PA} = \frac{\sum_{t=1}^{t=h}\sum_{i=1}^{i=N_t} p_{i,t}}{300 \times 3956} \quad (1)$$

$$PF = \frac{\sum_{t=1}^{t=h} N_t}{300 \times 3956} \quad (2)$$

$$PI = \frac{\sum_{t=1}^{t=h} \sum_{i=1}^{i=N_t} p_{i,t}}{\sum_{t=1}^{t=h} N_t} \quad (3)$$

It can be noted that PA is the product of PF and PI. The normalized diurnal variations of PA, PF, and PI are calculated by subtracting the daily mean from the value at each hour of a day and then dividing by the daily mean (Yu et al., 2007). The total precipitation hours and total precipitation at i station during RPE in the 43 summers are denoted by h_i and p_i. The total hours in the 43 summers are $h_t = 94944$ (24 hr × 92 days/summer × 43 summers). The PA, PF, and PI for the i station during RPE are defined by $\frac{p_i}{h_t}$, $\frac{h_i}{h_t}$, $\frac{p_i}{h_i}$, respectively.

2.3. Calculation of the Frontogenesis Function

The frontogenesis function is a physical quantity that quantifies the effects of atmospheric horizontal movement, vertical movement, and diabatic heating changes on frontogenesis (Hu et al., 2022; Thomas & Schultz, 2019; Xue et al., 2025). It can represent the change rate of the horizontal gradient of equivalent potential temperature θ_e with atmospheric mass point motion, effectively characterizing the structure and intensity of the front. Referring to Miller's theory (Miller, 1948), the frontogenesis function is decomposed into four terms, and the equations are as follows:

$$F_h = \frac{d}{dt}|\nabla_h \theta_e| = F1 + F2 + F3 + F4 \quad (4)$$

$$F1 = -\frac{1}{2} D |\nabla_h \theta_e| \quad (5)$$

$$F2 = -\frac{1}{2} \frac{E\left(\frac{\partial \theta_e}{\partial x}\right)^2 + 2F\left(\frac{\partial \theta_e}{\partial x}\right)\left(\frac{\partial \theta_e}{\partial y}\right) - E\left(\frac{\partial \theta_e}{\partial y}\right)^2}{|\nabla_h \theta_e|} \quad (6)$$

$$F3 = -\frac{\left(\frac{\partial \omega}{\partial x}\frac{\partial \theta_e}{\partial x} + \frac{\partial \omega}{\partial y}\frac{\partial \theta_e}{\partial y}\right)\frac{\partial \theta_e}{\partial p}}{|\nabla_h \theta_e|} \quad (7)$$

$$F4 = \frac{\frac{\partial \theta_e}{\partial x}\frac{\partial}{\partial x}\left(\frac{d\theta_e}{dt}\right) + \frac{\partial \theta_e}{\partial y}\frac{\partial}{\partial y}\left(\frac{d\theta_e}{dt}\right)}{|\nabla_h \theta_e|} \quad (8)$$

Where $F1$, $F2$, $F3$, $F4$ represent the divergence term, deformation term, tilting term, and diabatic heating term, respectively. $D = \frac{\partial u}{\partial x} + \frac{\partial v}{\partial y}$ denotes horizontal divergence in Equation 5, and $E = \frac{\partial u}{\partial x} - \frac{\partial v}{vy}$ and $F = \frac{\partial v}{\partial x} + \frac{\partial u}{vy}$ denote stretching and shear deformation in Equation 6.

3. Results

3.1. Characteristics of Diurnal Variation of RPE

During the summers from 1980 to 2022, RPE over MLYRB occurred under two monsoonal synoptic types (Type1: 8605 hr; Type2: 8456 hr) and the landfalling tropical cyclone synoptic type (Wu et al., 2025). Figure 1 shows that the spatial distribution and diurnal variations of PA, PF and PI for RPE over MLYRB in summer under Type1 and Type2. The RPE under Type1 and Type2 is concentrated over the southern and northern MLYRB (PA ≥ 0.07 mm/h), respectively, and PI and PF jointly determine the spatial distribution of PA (Figures 1a–1f). The PA of RPE over the northern MLYRB under Type2 is comparable to that over the southern MLYRB under Type1 (Figures 1a and 1b), but the PF (PI) is lower (higher) under Type2 than under Type1 (Figures 1c–1f). The PA of RPE under Type1 and Type2 is relatively higher from 05:00 to 12:00 LST in a day (Figures 1g and 1h), and the diurnal variations of PF and PI under Type1 and Type2 also exhibit a pronounced morning peak, but the peak of PF occurs 2 or 3 hours earlier than that of PI, as reported in previous studies (Chen et al., 2016; Jiang

et al., 2017). In addition, RPE under the landfalling tropical cyclone synoptic type primarily occur in the eastern MLYRB, and the diurnal variation shows late afternoon peak (Figure S1 in Supporting Information S1). Given the RPE associated with two monsoonal synoptic types occurring significantly more frequently, accounting for over 90% of occurrences of RPE, we concentrate on discussing in detail the formation mechanisms of diurnal variations of RPE under two monsoonal synoptic types. It should be emphasized that RPE under Type1 and Type2 contributes approximately 94% of the morning peak of total precipitation (Figure S2 in Supporting Information S1), and thus the mechanism discussed in this study remains robust for explaining the morning peak of total precipitation. Based on hourly (00:00-23:00 LST) composite analyses of environmental fields during RPE, the subsequent sections focus on the key factors regulating the diurnal variation of precipitation intensity.

3.2. Factors Regulating the Morning Peak of RPE

The low-level wind field is closely related to the diurnal variation of precipitation (Du & Chen, 2018; Liu et al., 2023), so we analyzed the spatial distribution and diurnal variation of wind at 850 hPa in Figure 2. Two monsoonal synoptic types exhibit pronounced southwesterly low-level jet (SLLJ; represented by the black box in Figures 2a and 2b) extending from South China to MLYRB with maximum wind speed exceeding 9 m/s, but their intensity and location differ significantly. The wind speed of SLLJ is stronger under Type2 than under Type1, bringing more abundant moisture and consequently resulting in higher PI (Figures 1e and 1f). The stronger SLLJ under Type2 is located to the northwest of that under Type1, pushing the precipitation belt farther northward (Figures 1a and 1b). The diurnal variation phases of the zonal and meridional winds of the SLLJ are not synchronized. Specifically, the zonal (meridional) wind starts to accelerate around 21:00 (18:00) LST and peaks at approximately 06:00 (03:00) LST (Figures 2c and 2d), and the vertical profile of SLLJ exhibits pronounced convex structure at 850 hPa from midnight to morning (Figure S3 in Supporting Information S1). The peaks of zonal and meridional winds occur several hours earlier than the morning peak of RPE. Notably, the strong zonal wind can persist until 09:00 LST before weakening significantly, which is closer to the morning peak of RPE. The enhanced meridional wind at midnight transports abundant moisture northward to MLYRB and promotes the development of moist convection (Fu et al., 2019). Moreover, the diurnal variation of SLLJ is dominated by its ageostrophic component, especially during the nocturnal acceleration of wind speed (Figure S4 in Supporting Information S1), which further demonstrates the critical role of ageostrophic wind induced by inertial oscillation in the morning peak of precipitation (Blackadar, 1957). The zonal geostrophic wind exhibits two diurnal cycles (Figures S4a and S4b in Supporting Information S1), which is closely related to the large-scale circulation forcing according to geostrophic balance theory. Interestingly, the diurnal variation of zonal movement of western Pacific subtropical high (WPSH) is found to be similar to that of the zonal geostrophic wind (Figure S5 in Supporting Information S1), and the possible mechanisms are preliminarily discussed. The first eastward retreat of WPSH (23:00-04:00 LST) is caused by the decrease in geopotential height due to atmospheric cooling at night (Figures S6a–S6e in Supporting Information S1). The first westward extension of WPSH (05:00-10:00 LST) is driven by downward solar radiation (Figures S5f–S5k in Supporting Information S1). When the land surface begins to heat up, the warming of the lower atmosphere induces stratification instability, which weakens the subsidence on the western side of WPSH and forces its second eastward retreat (11:00-16:00 LST). As atmospheric heat is transported vertically upward, warming in the middle troposphere causes second westward extension of WPSH (17:00-22:00 LST, Figures S6r–S6w in Supporting Information S1). The westward extension of WPSH in the morning increases the meridional pressure gradient on its northeastern side, thereby strengthening the zonal geostrophic wind. It should be noted that the wind field from the ERA5 exhibits discontinuities at 05:00 and 17:00 LST, attributable to the 12-hour assimilation window (09:00-21:00 and 21:00-09:00 UTC) employed by ERA5 (Hersbach et al., 2020). Multiple reanalysis data and observational data indicate that the ERA5 reanalysis data can accurately reproduce the true diurnal variations in wind (Cui et al., 2023; He et al., 2016; Xue et al., 2018), so the data discontinuity does not affect the robustness of the conclusions.

Under Type1 and Type2, there is significant horizontal wind shear associated with the cyclonic transition from southwesterly to easterly wind over MLYRB (Figures 2a and 2b). Relative vorticity is used to quantify the intensity of horizontal wind shear, which shows a distinct morning peak consistent with RPE (Figures 2e and 2f). The enhanced southwesterly and northeasterly winds on the southern and northern sides of MLYRB in the morning result in the strongest horizontal wind shear (Figure S7 in Supporting Information S1). In addition, the diurnal variation of relative vorticity is predominantly controlled by the meridional gradient of the zonal wind. Some studies on the impact of low-level jet on precipitation have mainly focused on the role of meridional wind

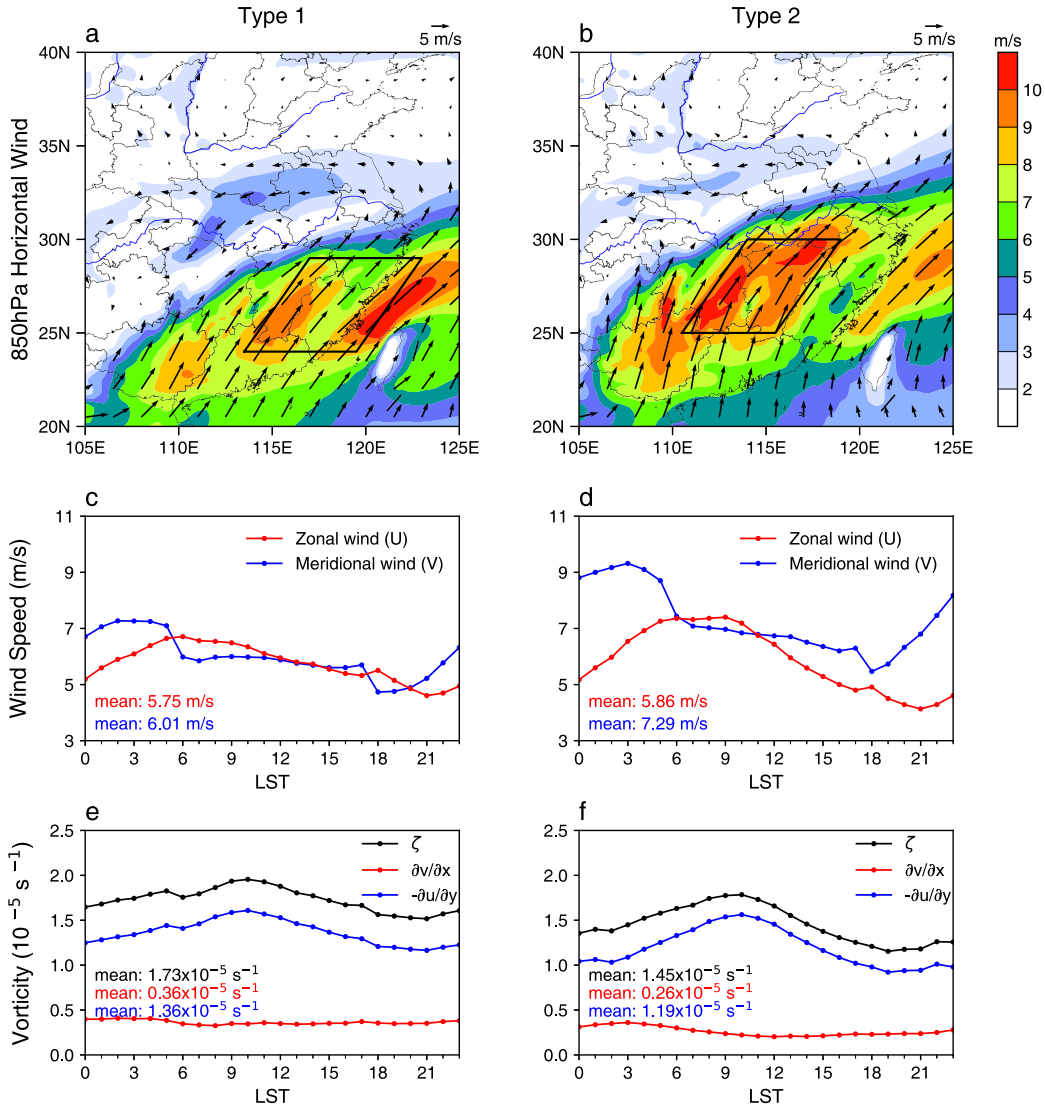

Figure 2. The spatial distribution of the composite mean horizontal wind field (vector) and wind speed (shading, unit: m/s) at 850 hPa in summers of 1980–2022 during the RPE under Type1 and Type2, respectively. The black box indicates the southwesterly low-level jet associated with the synoptic type (a, b). The diurnal variations of regional mean zonal (U) and meridional (V) winds in the black boxes of (a, b) during the RPE under Type1 and Type2, respectively (c, d). The diurnal variations of the relative vorticity at 850 hPa and its components regionally averaged over MLYRB (e, f). The daily means of variables are indicated by the values in the lower left corner of the subplots (c–f).

(Dong et al., 2021; Zeng et al., 2022), whereas this study complements the understanding of the role of zonal wind in regulating the morning peak of precipitation under specific synoptic types. Figure 3 shows the diurnal variations of vertical structure over MLYRB during RPE under the two monsoonal synoptic types. The convergence tilts northward with height, with the centers of convergence at low level located at 29°N and 31°N under Type1 and Type2, respectively (Figure 3a–3f). There is a typical configuration over MLYRB characterized by convergence in the low troposphere and divergence in the high troposphere, accompanied by strong ascending motion in the middle troposphere (Figures 3a–3f). Coupled with the nocturnal acceleration of SLLJ and the morning westward extension of WPSH, low-tropospheric convergence, mid-tropospheric ascending motion, and vertically integrated moisture convergence all exhibit pronounced morning peaks (Figure 3 and Figure S8 in Supporting Information S1). The vertical profile of divergence indicates that the precipitation system develops vertically at night, reaches its strongest and deepest stage at around 10:00 LST, and then gradually weakens

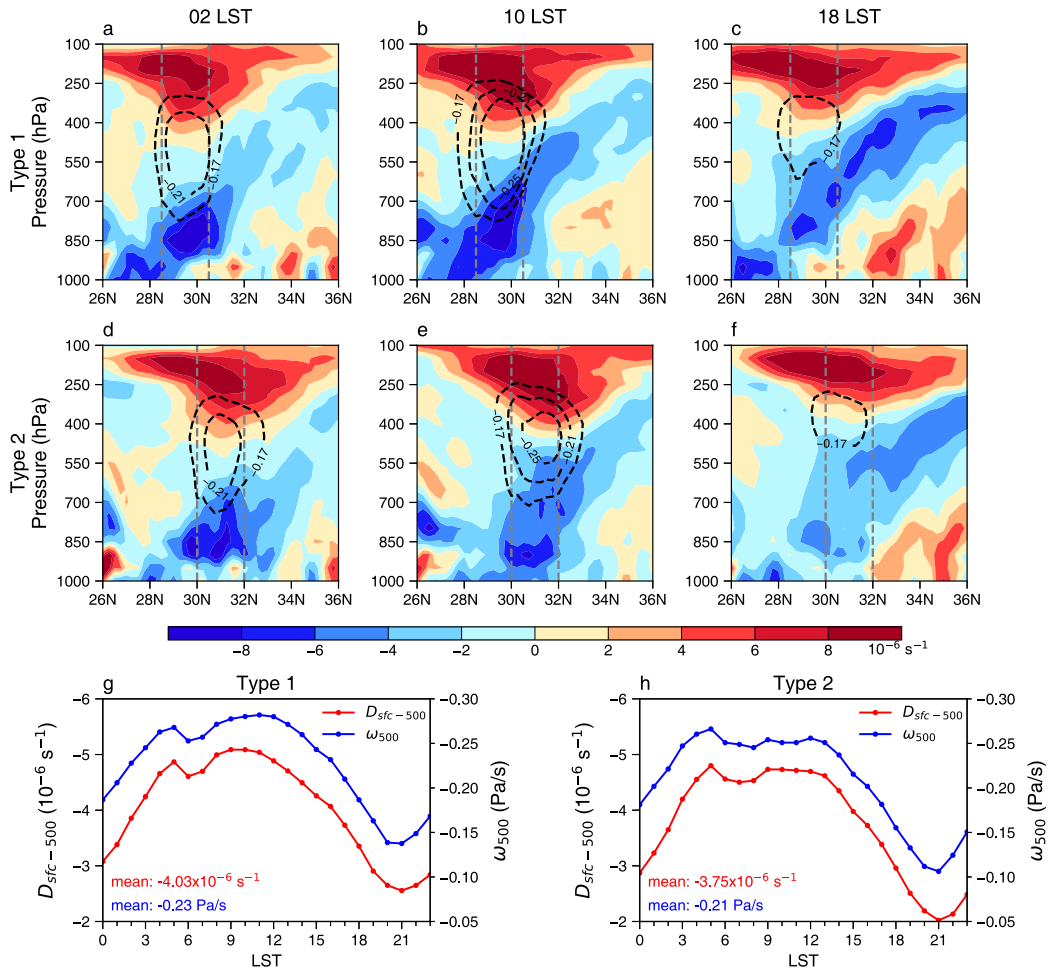

Figure 3. Pressure-latitude cross sections of the divergence (shading unit: 10^{-6} s^{-1}), and vertical velocity (black contour, unit: Pa/s) averaged along 110–122°E at 02:00, 10:00 and 18:00 LST during the RPE under Type1 and Type2 (a–f). The diurnal variations of vertically mean divergence from surface to 500 hPa and vertical velocity at 500 hPa in the gray box region under Type1 (28.5–30.5°N) and Type2 (30–32°N) (g, h). Their daily means are shown in the lower left corner.

(Figures 3a–3f). Overall, the strongest horizontal wind shear, convergence and ascending motion mark the most mature stage of the convective system, leading to the morning peak of precipitation.

RPE over the MLYRB in summer are often accompanied by pronounced frontogenesis, which arises from the synergistic interaction of multi-scale synoptic systems, including WPSH, SLLJ, and mesoscale vortices (Chen et al., 2007; Du et al., 2014; Liu et al., 2023; Zhang et al., 2018). Under the two monsoonal synoptic types, the warm and moist airflow on the northwestern flank of WPSH and mid-latitude dry and cold air converge over MLYRB, forming a dense belt of equivalent potential temperature (frontal zone; horizontal gradient >3 K/100 km) at 850 hPa over the southern and northern MLYRB, respectively (Figure S9 in Supporting Information S1). The frontogenesis function can effectively modulate precipitation variation over MLYRB through combined dynamic and thermodynamic effects (Hou & Guan, 2013; Jiang et al., 2025). The diabatic heating and tilting terms within the frontal zone collectively exhibit frontolysis with their diurnal variations concentrated mainly in the afternoon (Figure S10 in Supporting Information S1). Following the method of Hu et al. (2021), we further decompose the diabatic heating term into new diabatic heating term, moisture change term, and lifting condensation temperature change term. It is found that the new diabatic heating term dominates frontogenesis, while the moisture change term produces a stronger frontolysis magnitude (Figures S11a–S11d in Supporting Information S1), resulting in frontolysis for the diabatic heating term (Figures S10a and S10b in Supporting Information S1). Since the diurnal variations of these components are concentrated in the afternoon, we suggest that the diabatic heating and tilting terms have relatively limited direct impacts on

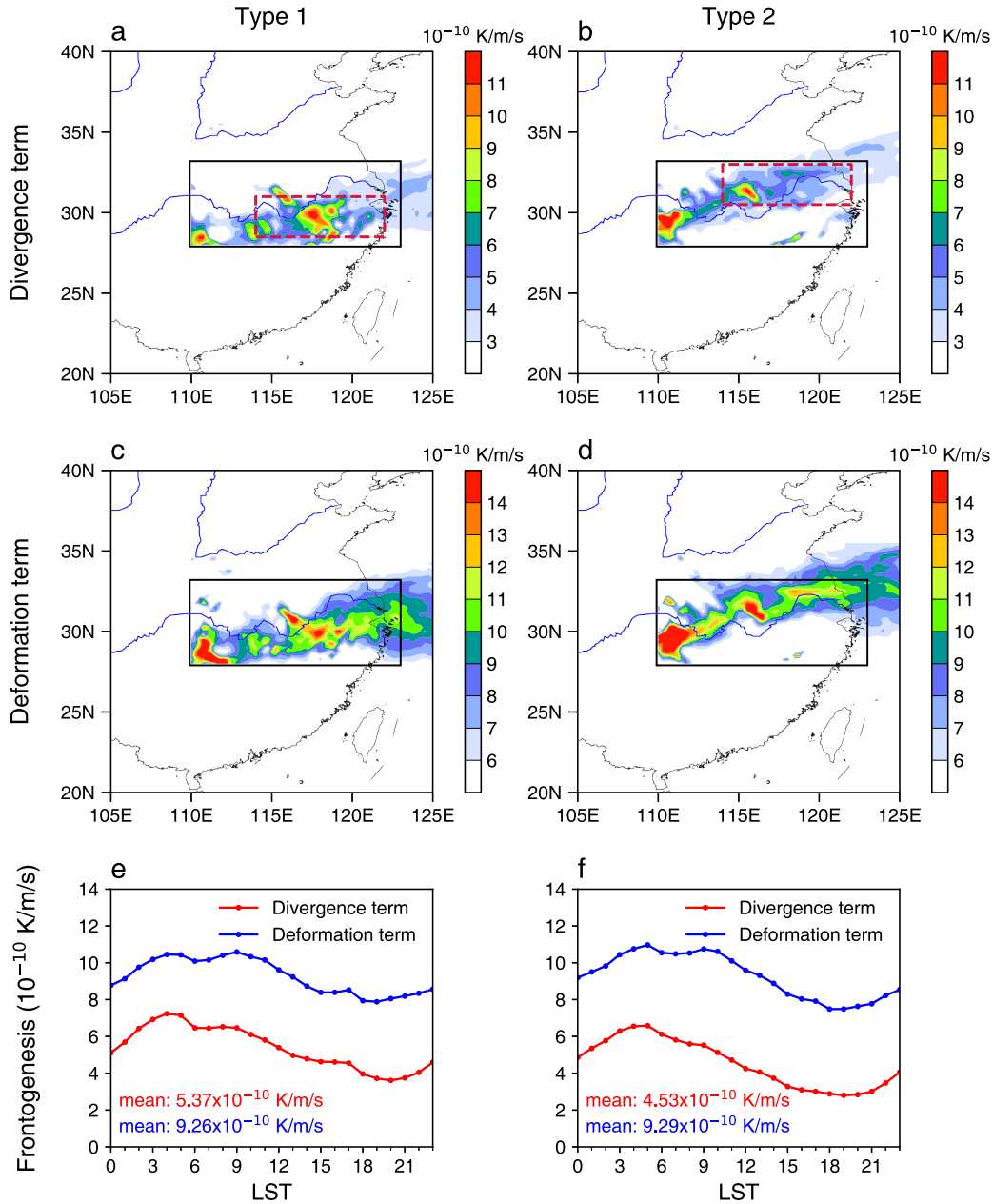

Figure 4. The spatial distribution of the composite mean divergence frontogenesis (a, b) and deformation frontogenesis (c, d) (unit: 10^{-10} K/m/s) at 850 hPa during the RPE under Type1 and Type2. The diurnal variations of deformation frontogenesis and divergence frontogenesis at 850 hPa in the red boxes of (a, b) under Type1 and Type2. Their daily means are shown in the lower left corner (e, f).

the morning peak of precipitation. The divergence frontogenesis and deformation frontogenesis largely coincide with the frontal zone (Figures 4a–4d), and they are the primary contributors to frontogenesis in the lower troposphere, as previously reported (Jin et al., 2023; Yang et al., 2015). However, the magnitude of deformation frontogenesis is significantly greater than that of divergence frontogenesis, with maximum values reaching up to 1.4×10^{-9} K/m/s. The diurnal variations of divergence frontogenesis and deformation frontogenesis exhibit unimodal structure, and the peaks occur at night and in the morning, respectively (Figures 4e and 4f). In the morning, the SLLJ and WPSH force significant stretching and shearing deformations in the low-level wind field, thereby driving the deformation frontogenesis to reach its peak. Both the magnitude and

diurnal variation phase indicate that deformation frontogenesis plays a more important role than divergence frontogenesis in regulating the diurnal variation of RPE.

4. Conclusion and Discussion

In this study, we investigate the regulatory factors of the morning peak of RPE over MLYRB in the summers from 1980 to 2022. The PA, PF and PI of RPE over MLYRB associated with two monsoon synoptic types (Type1 and Type2) all exhibit pronounced morning peaks. The results indicate that both Type1 and Type2 exhibit SLLJ, and significant differences exist in their intensity and location, leading to distinct precipitation intensity and spatial distribution. Both the zonal and meridional winds of SLLJ begin to accelerate at night and reach their peaks before the morning peak of precipitation, but the meridional wind peaks (around 06:00 LST) approximately 3 hr later than the zonal wind (around 03:00 LST). The ageostrophic wind dominates the diurnal variation of SLLJ, particularly the nocturnal acceleration of ageostrophic wind promote the development of precipitation systems. Moreover, the westward expansion of WPSH in the morning facilitates the development of the zonal geostrophic wind, providing a large-scale synoptic forcing background for the morning peak of precipitation. The coupling between SLLJ acceleration and WPSH westward extension produces the strongest low-level relative vorticity, convergence, and mid-level ascending motion in the morning, indicating that the precipitation system develops to its most mature stage. In addition, RPE are associated with pronounced frontogenesis over the southern and northern MLYRB under Type 1 and Type 2, respectively. The deformation frontogenesis plays a dominant role in regulating the morning peak of RPE, followed by divergence frontogenesis, whereas diabatic heating frontogenesis and tilting frontogenesis exert negligible influence on the morning peak.

Compared with previous studies, this study deepens our understanding of the crucial role of zonal winds in regulating the morning peak of precipitation under specific synoptic patterns, and provides important supplementary insights into the influence of frontogenesis on the diurnal variation of precipitation. The lag difference in peak phase between precipitation frequency and precipitation intensity may be attributed to the asymmetric evolution of precipitation processes and convective cloud systems (Yu et al., 2013; Yu & Li, 2016). As nocturnal SLLJ accelerates, widespread stratiform precipitation and shallow convection develop first, expanding precipitation coverage and increasing precipitation station count (PSC), which makes PF peak in advance (Figure S12 in Supporting Information S1). Subsequently, the precipitation system develops vertically and evolves gradually into deep convection, resulting in a slight shrinkage of the precipitation coverage and a corresponding decrease in PSC, thereby enabling PI to reach its peak several hours after the peak of PF. In the future, higher-resolution data and numerical models will be needed to further investigate the underlying physical mechanisms of precipitation asymmetry.

Conflict of Interest

The authors declare no conflicts of interest relevant to this study.

Availability Statement

Precipitation observation data can be obtained from CMA (2026). The hourly geopotential height, specific humidity, temperature, vertical velocity, meridional wind and zonal wind are accessed from ERA5 (Hersbach et al., 2020). The data and code used to generate the results in this study have been published in Wu (2026).

Acknowledgments
This study is funded by the National Natural Science Foundation of China under Grants U2342207, the Open Project Fund of China Meteorological Administration Basin Heavy Rainfall Key Laboratory (Grant. 2023BHR-Z01), and the Jiangsu Collaborative Innovation Center for Climate Change. We sincerely thank the three anonymous reviewers for their constructive and valuable comments and suggestions.

References

Ali, H., & Mishra, V. (2018). Contributions of dynamic and thermodynamic scaling in subdaily precipitation extremes in India. *Geophysical Research Letters*, *45*(5), 2352–2361. https://doi.org/10.1002/2018gl077065

Blackadar, A. K. (1957). Boundary layer wind maxima and their significance for the growth of nocturnal inversions. *Bulletin of the American Meteorological Society*, *38*(5), 283–290. https://doi.org/10.1175/1520-0477-38.5.283

Cao, F. Q., Gao, T., Dan, L., Ma, Z. G., Chen, X. L., Zou, L. W., & Zhang, L. (2019). Synoptic-scale atmospheric circulation anomalies associated with summertime daily precipitation extremes in the middle-lower reaches of the Yangtze River Basin. *Climate Dynamics*, *53*(5–6), 3109–3129. https://doi.org/10.1007/s00382-019-04687-3

Chen, G. T. J., Wang, C. C., & Wang, A. H. (2007). A case study of subtropical frontogenesis during a blocking event. *Monthly Weather Review*, *135*(7), 2588–2609. https://doi.org/10.1175/mwr3412.1

Chen, H. M., Yuan, W. H., Li, J., & Yu, R. C. (2012). A possible cause for different diurnal variations of warm season rainfall as shown in station observations and TRMM 3B42 data over the southeastern Tibetan plateau. *Advances in Atmospheric Sciences*, *29*(1), 193–200. https://doi.org/10.1007/s00376-011-0218-1

Chen, P. H., Chen, A. F., Yin, S. Q., Li, Y. X., & Liu, J. G. (2024). Clustering the diurnal cycle of precipitation using global satellite data. *Geophysical Research Letters*, *51*(23), e2024GL111513. https://doi.org/10.1029/2024gl111513

Chen, S., Behrangi, A., Tian, Y. D., Hu, J. J., Hong, Y., Tang, Q. H., et al. (2016). Precipitation Spectra analysis over China with high-resolution measurements from optimally-merged Satellite/Gauge observations-part II: Diurnal variability analysis. *Ieee Journal of Selected Topics in Applied Earth Observations and Remote Sensing*, *9*(7), 2979–2988. https://doi.org/10.1109/jstars.2016.2529001

CMA. (2026). China surface meteorological observation data [Dataset]. Retrieved from https://data.cma.cn/data/detail/dataCode/A.0012.0001.S011.html

Cui, C. G., Zhou, W., Yang, H., Wang, X. K., Deng, Y., Wang, X. F., et al. (2023). Analysis of the characteristics of the low-level jets in the middle reaches of the Yangtze River during the Mei-yu season. *Advances in Atmospheric Sciences*, *40*(4), 711–724. https://doi.org/10.1007/s00376-022-2107-1

Dai, A. G. (2024). The diurnal cycle from observations and ERA5 in precipitation, clouds, boundary layer height, buoyancy, and surface fluxes. *Climate Dynamics*, *62*(7), 5879–5908. https://doi.org/10.1007/s00382-024-07182-6

Dong, F., Zhi, X. F., Zhang, L., & Ye, C. Z. (2021). Diurnal variations of coastal boundary layer jets over the Northern South China Sea and their impacts on diurnal cycle of rainfall over Southern China during the early-summer rainy season. *Monthly Weather Review*, *149*(10), 3341–3363. https://doi.org/10.1175/mwr-d-20-0292.1

Du, Y., & Chen, G. X. (2018). Heavy rainfall associated with double low-level jets over Southern China. Part I: Ensemble-based analysis. *Monthly Weather Review*, *146*(11), 3827–3844. https://doi.org/10.1175/mwr-d-18-0101.1

Du, Y., Xie, Z. Q., & Miao, Q. (2020). Spatial scales of heavy meiyu precipitation events in Eastern China and associated atmospheric processes. *Geophysical Research Letters*, *47*(11), e2020GL087086. https://doi.org/10.1029/2020gl087086

Du, Y., Zhang, Q. H., Chen, Y. L., Zhao, Y. Y., & Wang, X. (2014). Numerical simulations of spatial distributions and diurnal variations of low-level jets in China during early summer. *Journal of Climate*, *27*(15), 5747–5767. https://doi.org/10.1175/jcli-d-13-00571.1

Fu, P. L., Zhu, K. F., Zhao, K., Zhou, B. W., & Xue, M. (2019). Role of the nocturnal low-level jet in the Formation of the morning precipitation peak over the Dabie Mountains. *Advances in Atmospheric Sciences*, *36*(1), 15–28. https://doi.org/10.1007/s00376-018-8095-5

Gong, J., Zeng, X. P., Wu, D. L., & Li, X. W. (2018). Diurnal variation of tropical ice cloud microphysics: Evidence from global precipitation measurement Microwave imager polarimetric measurements. *Geophysical Research Letters*, *45*(2), 1185–1193. https://doi.org/10.1002/2017gl075519

Guan, P. Y., Chen, G. X., Zeng, W. X., & Liu, Q. (2020). Corridors of mei-yu-season rainfall over Eastern China. *Journal of Climate*, *33*(7), 2603–2626. https://doi.org/10.1175/jcli-d-19-0649.1

Hayden, L., & Liu, C. T. (2021). Differences in the diurnal variation of precipitation estimated by spaceborne radar, passive microwave radiometer, and IMERG. *Journal of Geophysical Research-Atmospheres*, *126*(9), e2020JD033020. https://doi.org/10.1029/2020jd033020

He, M. Y., Liu, H. B., Wang, B., & Zhang, D. L. (2016). A modeling Study of a low-level jet along the Yun-Gui Plateau in south China. *Journal of Applied Meteorology and Climatology*, *55*(1), 41–60. https://doi.org/10.1175/jamc-d-15-0067.1

Hersbach, H., Bell, B., Berrisford, P., Hirahara, S., Horányi, A., Muñoz-Sabater, J., et al. (2020). The ERA5 global reanalysis [Dataset]. *Quarterly Journal of the Royal Meteorological Society*, *146*(730), 1999–2049. https://doi.org/10.1002/qj.3803

Hou, J., & Guan, Z. Y. (2013). Climatological characteristics of frontogenesis and related circulations over East China in June and July. *Acta Meteorologica Sinica*, *27*(2), 144–169. https://doi.org/10.1007/s13351-013-0202-z

Hu, Y., Deng, Y., Lin, Y. L., Zhou, Z. M., Cui, C. G., & Dong, X. Q. (2021). Dynamics of the spatiotemporal morphology of Mei-yu fronts: An initial survey. *Climate Dynamics*, *56*(9–10), 2715–2728. https://doi.org/10.1007/s00382-020-05619-2

Hu, Y., Deng, Y., Lin, Y. L., Zhou, Z. M., Cui, C. G., Li, C., & Dong, X. (2022). Indirect effect of diabatic heating on Mei-yu frontogenesis. *Climate Dynamics*, *59*(3–4), 851–868. https://doi.org/10.1007/s00382-022-06159-7

Jiang, Y. Q., Yin, Y. X., Li, W. T., Dai, S. B., Long, X. J., & Jiao, Y. (2025). Weather pattern classification of regional extreme precipitation events and their formation mechanisms in the Yangtze-Huai Region, China. *Climate Dynamics*, *63*(1), 39. https://doi.org/10.1007/s00382-024-07532-4

Jiang, Z. N., Zhang, D. L., Xia, R. D., & Qian, T. T. (2017). Diurnal variations of presummer rainfall over Southern China. *Journal of Climate*, *30*(2), 755–773. https://doi.org/10.1175/jcli-d-15-0666.1

Jin, X., Liu, M., Li, Y., Wang, L., Li, C., & Chen, W. (2023). Analysis of the frontogenesis characteristics of different types of rainstorms in the Jianghuai Meiyu period. *Transactions of Atmospheric Sciences*, *46*(4), 600–614. https://doi.org/10.13878/j.cnki.dqkxxb.20220727001

Li, C., Cui, C. G., Jiang, X. W., Wang, X. F., Fu, S. M., Cui, W. J., et al. (2024). Diurnal variation in short- and long-duration precipitation within the Dabie Mountain region in Central China. *International Journal of Climatology*, *44*(5), 1277–1301. https://doi.org/10.1002/joc.8333

Li, X. Y., & Lu, R. Y. (2018). Subseasonal change in the seesaw pattern of precipitation between the Yangtze River Basin and the tropical Western north Pacific during summer. *Advances in Atmospheric Sciences*, *35*(10), 1231–1242. https://doi.org/10.1007/s00376-018-7304-6

Li, X. Y., Lu, R. Y., & Wang, X. D. (2023). Effect of large-scale circulation anomalies on summer rainfall over the Yangtze River Basin: Tropical versus extratropical. *Journal of Climate*, *36*(13), 4571–4587. https://doi.org/10.1175/jcli-d-22-0717.1

Liu, J. Z., Yang, L., Jiang, J. C., Yuan, W. H., & Duan, Z. (2021). Mapping diurnal cycles of precipitation over China through clustering. *Journal of Hydrology*, *592*, 125804. https://doi.org/10.1016/j.jhydrol.2020.125804

Liu, L. P., Ruan, Z., & Qin, D. Y. (2005). Case studies on mesoscale structures of heavy rainfall system in the Yangtze River generated by Meiyu front. *Science in China, Series D: Earth Sciences*, *48*(8), 1303–1311. https://doi.org/10.1360/03yd0319

Liu, X. Y., Chen, G. X., Zhang, S. J., & Du, Y. (2023). Formation of low-level jets over Southern China in the Mei-yu season. *Advances in Atmospheric Sciences*, *40*(10), 1731–1748. https://doi.org/10.1007/s00376-023-2358-5

Miller, J. E. (1948). ON the CONCEPT OF FRONTOGENESIS. *Journal of Meteorology*, *5*(4), 169–171. https://doi.org/10.1175/1520-0469(1948)005<0169:Otcof>2.0.Co;2

Minobe, S., Park, J. H., & Virts, K. S. (2020). Diurnal cycles of precipitation and lightning in the tropics observed by TRMM3G68, GSMaP, LIS, and WWLLN. *Journal of Climate*, *33*(10), 4293–4313. https://doi.org/10.1175/jcli-d-19-0389.1

Nesbitt, S. W., & Zipser, E. J. (2003). The diurnal cycle of rainfall and convective intensity according to three years of TRMM measurements. *Journal of Climate*, *16*(10), 1456–1475. https://doi.org/10.1175/1520-0442-16.10.1456

Pan, H., & Chen, G. X. (2019). Diurnal variations of precipitation over North China regulated by the mountain-plains solenoid and boundary-layer inertial oscillation. *Advances in Atmospheric Sciences*, *36*(8), 863–884. https://doi.org/10.1007/s00376-019-8238-3

Pan, X., Fu, Y. F., Yang, S., Gong, Y., & Li, D. Q. (2021). Diurnal variations of precipitation over the steep slopes of the himalayas observed by TRMM PR and VIRS. *Advances in Atmospheric Sciences*, *38*(4), 641–660. https://doi.org/10.1007/s00376-020-0246-9

Qiao, F. X., & Liang, X. Z. (2016). Effects of cumulus parameterization closures on simulations of summer precipitation over the United States coastal oceans. *Journal of Advances in Modeling Earth Systems*, *8*(2), 764–785. https://doi.org/10.1002/2015ms000621

Rickenbach, T. M., Nieto-Ferreira, R., Zarzar, C., & Nelson, B. (2015). A seasonal and diurnal climatology of precipitation organization in the southeastern United States. *Quarterly Journal of the Royal Meteorological Society*, *141*(690), 1938–1956. https://doi.org/10.1002/qj.2500

Ruane, A. C. (2010). NARR's atmospheric water cycle components. Part II: Summertime mean and diurnal interactions. *Journal of Hydrometeorology*, *11*(6), 1220–1233. https://doi.org/10.1175/2010jhm1279.1

Song, J. Y., Song, F. F., Feng, Z., Leung, L. R., Li, C., & Wu, L. X. (2024). Realistic precipitation diurnal cycle in global convection-permitting models by resolving mesoscale convective systems. *Geophysical Research Letters*, *51*(13), e2024GL109945. https://doi.org/10.1029/2024gl109945

Sui, X. X., Yang, Z. L., & Niyogi, D. (2025). Diurnal urban rainfall anomalies across different landscapes. *Science Advances*, *11*(33), eads5046. https://doi.org/10.1126/sciadv.ads5046

Tang, Y. L., Xu, G. R., Wan, R., & Wang, X. F. (2022). Characteristics of summer hourly precipitation under different urbanization background in central China. *Scientific Reports*, *12*(1), 7551. https://doi.org/10.1038/s41598-022-11487-z

Thomas, C. M., & Schultz, D. M. (2019). Global climatologies of fronts, airmass boundaries, and airstream boundaries: Why the definition of "Front" matters. *Monthly Weather Review*, *147*(2), 691–717. https://doi.org/10.1175/mwr-d-18-0289.1

Wang, X. F., Cui, C. G., Cui, W. J., & Shi, Y. (2014). Modes of mesoscale convective System Organization during Meiyu season over the Yangtze River Basin. *Journal of Meteorological Research*, *28*(1), 111–126. https://doi.org/10.1007/s13351-014-0108-4

Wu, R. (2026). Regulatory factors of the morning peak of summer regional precipitation events over the middle and lower Yangtze River Basin, China [Dataset]. *Zenodo*. https://doi.org/10.5281/zenodo.19479497

Wu, R., Huang, A., Huang, D., Tang, J., & Xu, X. (2025). Characteristics of the summer regional precipitation events in the middle and lower Yangtze River Basin and associated mechanisms. *Journal of Geophysical Research: Atmospheres*, *130*(3), e2024JD042622. https://doi.org/10.1029/2024JD042622

Wu, Y., Huang, A. N., Huang, D. Q., Chen, F., Yang, B., Zhou, Y., et al. (2018). Diurnal variations of summer precipitation over the regions east to Tibetan Plateau. *Climate Dynamics*, *51*(11–12), 4287–4307. https://doi.org/10.1007/s00382-017-4042-x

Xue, M., Luo, X., Zhu, K. F., Sun, Z. Q., & Fei, J. F. (2018). The controlling role of boundary layer inertial oscillations in Meiyu frontal precipitation and its diurnal cycles over China. *Journal of Geophysical Research-Atmospheres*, *123*(10), 5090–5115. https://doi.org/10.1029/2018jd028368

Xue, Y. D., Yao, S. X., & Huang, Q. (2025). Mechanistic diversity of hourly extreme rainfall in the middle and lower reaches of the Yangtze River Basin. *Journal of Geophysical Research-Atmospheres*, *130*(15), e2025JD043729. https://doi.org/10.1029/2025jd043729

Yang, R. Y., Zhang, Y. C., Sun, J. H., & Li, J. (2020). The comparison of statistical features and synoptic circulations between the eastward-propagating and quasi-stationary MCSs during the warm season around the second-step terrain along the middle reaches of the Yangtze River. *Science China Earth Sciences*, *63*(8), 1209–1222. https://doi.org/10.1007/s11430-018-9385-3

Yang, S., Gao, S. T., & Lu, C. G. (2015). Investigation of the Mei-yu front using a new deformation frontogenesis function. *Advances in Atmospheric Sciences*, *32*(5), 635–647. https://doi.org/10.1007/s00376-014-4147-7

Yang, S., & Smith, E. A. (2008). Convective-stratiform precipitation variability at seasonal scale from 8 yr of TRMM observations: Implications for multiple modes of diurnal variability. *Journal of Climate*, *21*(16), 4087–4114. https://doi.org/10.1175/2008jcli2096.1

Yang, Y. H., Zhai, P. M., Li, J. Y., & Wang, Q. (2025). Rainbelt properties of persistent heavy precipitation over the Yangtze River Basin and associated three-dimensional circulations. *Weather and Forecasting*, *40*(5), 689–702. https://doi.org/10.1175/waf-d-24-0054.1

Yao, R., Zhang, S. L., Sun, P., Bian, Y. J., Yang, Q. Q., Guan, Z. K., & Zhang, Y. (2022). Diurnal variations in different precipitation duration events over the Yangtze River Delta urban agglomeration. *Remote Sensing*, *14*(20), 5244. https://doi.org/10.3390/rs14205244

Yu, R. C., Li, J., Chen, H. M., & Yuan, W. H. (2014). Progress in studies of the precipitation diurnal variation over contiguous China. *Journal of Meteorological Research*, *28*(5), 877–902. https://doi.org/10.1007/s13351-014-3272-7

Yu, R., & Li, J. (2016). Regional characteristics of diurnal peak phases of precipitation over contiguous China. *Acta Meteorologica Sinica*, *74*(1), 18–30. https://doi.org/10.11676/qxxb2016.011

Yu, R. C., Chen, H. M., & Sun, W. (2015). The definition and characteristics of regional rainfall events demonstrated by warm season precipitation over the Beijing Plain. *Journal of Hydrometeorology*, *16*(1), 396–406. https://doi.org/10.1175/jhm-d-14-0086.1

Yu, R. C., Xu, Y. P., Zhou, T. J., & Li, J. (2007). Relation between rainfall duration and diurnal variation in the warm season precipitation over central eastern China. *Geophysical Research Letters*, *34*(13). https://doi.org/10.1029/2007gl030315

Yu, R. C., Yuan, W. H., & Li, J. (2013). The asymmetry of rainfall process. *Chinese Science Bulletin*, *58*(16), 1850–1856. https://doi.org/10.1007/s11434-012-5653-6

Yuan, Z. P., Zhuge, X. Y., & Wang, Y. (2020). The forced secondary circulation of the Mei-yu front. *Advances in Atmospheric Sciences*, *37*(7), 766–780. https://doi.org/10.1007/s00376-020-9177-8

Zeng, J. W., Huang, A. N., Wu, P. L., Huang, D. Q., Zhang, Y., Tang, J., et al. (2023). Typical synoptic patterns responsible for summer regional hourly extreme precipitation events over the middle and lower Yangtze River Basin, China. *Geophysical Research Letters*, *50*(17), e2023GL104829. https://doi.org/10.1029/2023gl104829

Zeng, W. X., Chen, G. X., Bai, L. Q., Liu, Q., & Wen, Z. P. (2022). Multiscale processes of heavy rainfall over east Asia in summer 2020: Diurnal cycle in response to synoptic disturbances. *Monthly Weather Review*, *150*(6), 1355–1376. https://doi.org/10.1175/mwr-d-21-0308.1

Zeng, W. X., Chen, G. X., Du, Y., & Wen, Z. P. (2019). Diurnal variations of low-level winds and precipitation response to large-scale circulations during a heavy rainfall event. *Monthly Weather Review*, *147*(11), 3981–4004. https://doi.org/10.1175/mwr-d-19-0131.1

Zhang, F., Li, M. X., Zhang, Q. H., Liu, M., Xu, J., Guo, J. P., & Fan, H. (2025). Differences in triggering conditions between embedded and isolated convection initiation during a Meiyu season in China. *Quarterly Journal of the Royal Meteorological Society*, *151*(768), e4927. https://doi.org/10.1002/qj.4927

Zhang, F., Zhang, Q. H., Sun, J. Z., & Xu, J. (2023). Convection initiation during the meiyu environment in the Yangtze-Huai River Basin of China. *Journal of Geophysical Research-Atmospheres*, *128*(9), e2022JD038077. https://doi.org/10.1029/2022jd038077

Zhang, Y. C., & Sun, J. H. (2017). Comparison of the diurnal variations of precipitation east of the Tibetan Plateau among sub-periods of Meiyu season. *Meteorology and Atmospheric Physics*, *129*(5), 539–554. https://doi.org/10.1007/s00703-016-0484-7

Zhang, Y. C., Zhang, F. Q., Davis, C. A., & Sun, J. H. (2018). Diurnal evolution and structure of long-lived mesoscale convective vortices along the Mei-Yu front over the East China plains. *Journal of the Atmospheric Sciences*, *75*(3), 1005–1025. https://doi.org/10.1175/jas-d-17-0197.1